Supplementary Information

Creating Polymer Hydrogel Microfibres with Internal Alignment *via* Electrical and Mechanical Stretching

Shuming Zhang, Xi Liu, Sebastian F. Barreto-Ortiz, Yixuan Yu, Brian Ginn,

Nicholas DeSantis, Daphne L Hutton, Warren Grayson, Fu-Zhai Cui, Brian A. Korgel,

Sharon Gerecht and Hai-Quan Mao*

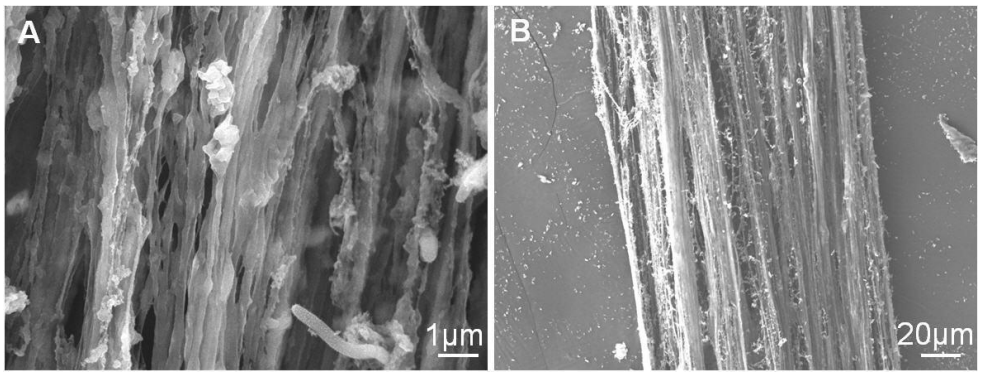

Fig. S1. SEM micrographs of dual component hydrogel fibres prepared with thiolated hyaluronic acid and gelatin. The dual component hydrogel fibres were prepared according to conditions listed in Table 1. Images reveal high degree of preferential alignment along the gel long axis, similar to the fibrin, gelatin and HA fibres reported in the main text.

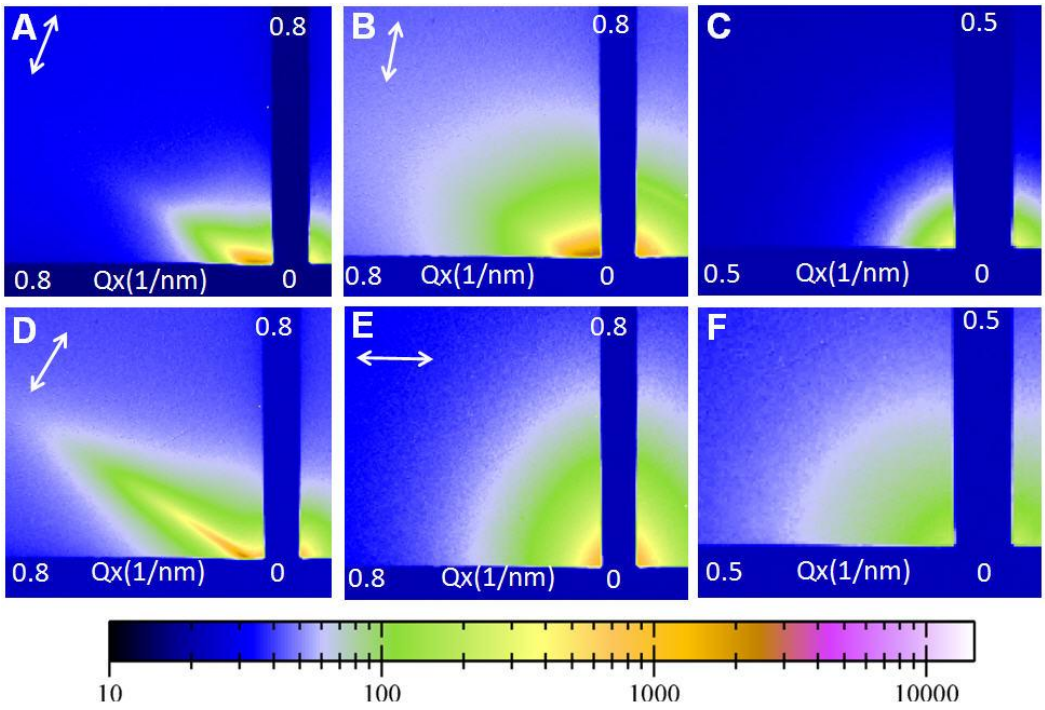

Fig. S2. Small angle x-ray scattering (SAXS) patterns for fibrin and gelatin hydrogel microfibres. (A-B) SAXS patterns of dry (A) and wet (B) fibrin hydrogel fibres prepared by electrostretching. (C) SAXS pattern for fibrin hydrogel samples prepared by simple extrusion. (D-E) SAXS patterns of dry (D) and wet (E) gelatin hydrogel fibres prepared by electrostretching. (F) SAXS pattern for gelatin hydrogel samples prepared by simple extrusion. These analyses, together with data shown in Fig. 3, confirm that hydrogel fibres prepared by electrostretching exhibit polymer chain alignment along the microfiber axis as indicated by the white arrows. In contrast, hydrogel samples prepared by simple extrusion have an isotropic structure.

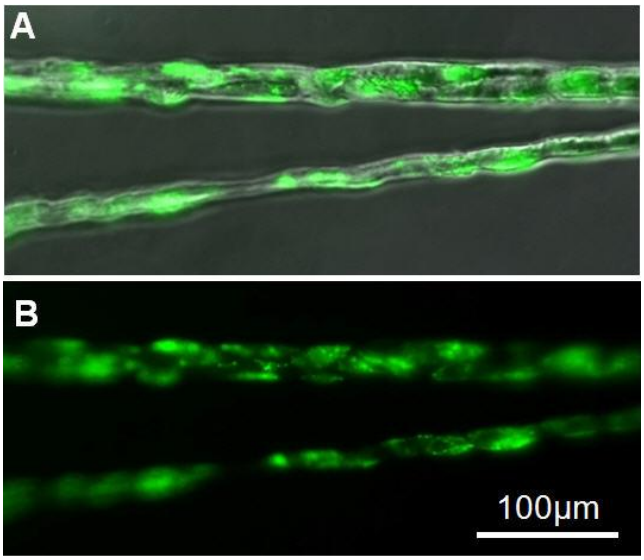

Fig. S3. Fluorescence images of human umbilical vein endothelial cells (HUVECs) cultured on the surface of fibrin-alginate microfibres. HUVECs were labeled with CellTracker^{TM} green CMFDA dye, seeded on fibrin microfibres, and cultured for 2 days in the maintenance medium. (A-B) Overlay (A) and fluorescence (B) images of the sample reveal a high degree of coverage on the microfibres after 2 days of culture.

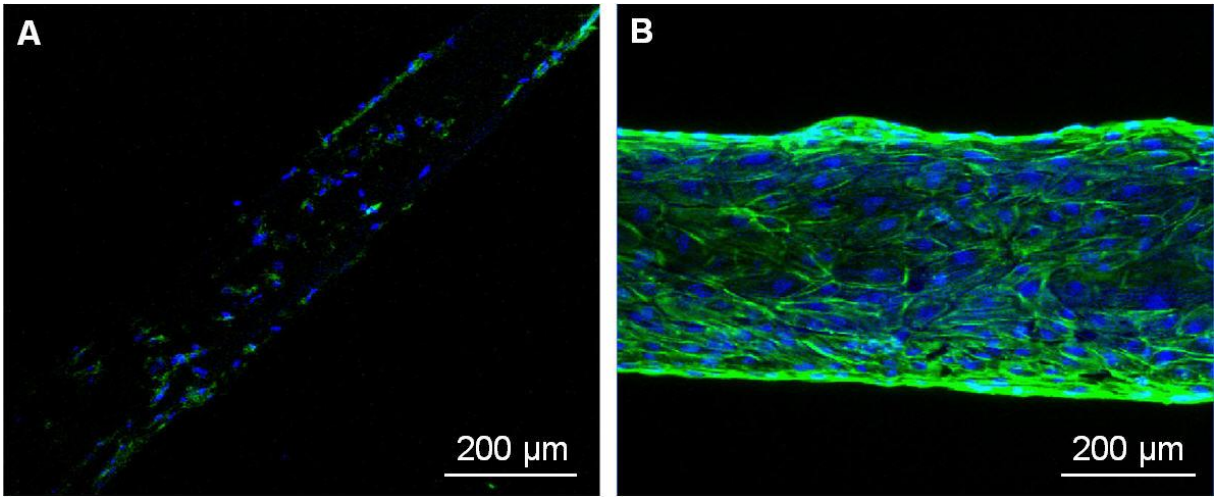

Fig. S4. Fluorescent imaging of ECFC proliferation on fibrin microfibres. Confocal z-stack image reconstructions of ECFCs seeded on fibrin microfibres after (a) 1 day and (b) 5 days in culture. Actin filaments (phalloidin staining) are shown in green and nuclei are counterstained in blue.

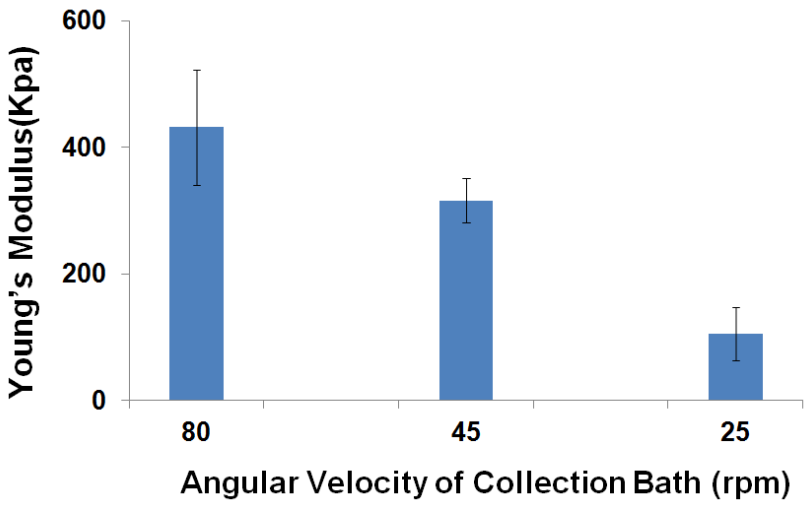

Fig. S5. Tensile moduli of wet alginate hydrogel fibres prepared at different rotation speeds. All fibre samples were crosslinked in 25 mM $CaCl_2$ solution for 4 min prior to measurement. The Young's modulus of the wet fibres increased with the angular velocity of the collection bath. These results suggest that a higher degree of mechanical stretching—under a higher angular velocity of the collection bath—induces a higher degree of polymer chain alignment, manifested by a higher Young's modulus. Although higher degree of alignment is achieved with smaller diameter hydrogel microfibers, it is easy to group individual fibres into a larger diameter fibre bundle while maintaining good alignment and mechanical properties.

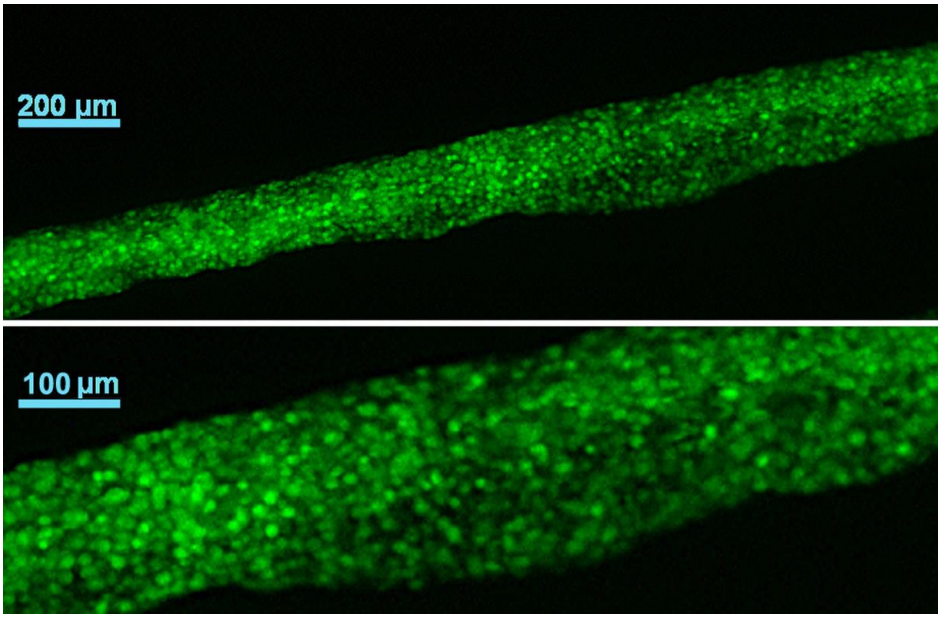

Fig. S6. Fluorescence images of human immortalized Schwann cells immediately following microfiber collection. Cells were seeded at a density of 22,000 cells per microliter of 0.4 wt% fibrinogen spinning solution under the conditions described in Table 1. Cells were labelled with CellTracker^{TM} green CMFDA dye. These images showed that cells did not spread and align as a result of electrical and mechanical stretching. Cell alignment and spreading were induced gradually as cells sensed the matrix alignment topography.